A Study on the Modeling of Magnetic Arc Deflection and Dynamic Analysis of Arc Sensor

A magnetic field applied to a welding arc produced an output signal beneficial for an arc sensor

BY Y. H. KANG AND S. J. NA

ABSTRACT. This investigation presents theoretical predictions and experimental results of the effect of a magnetic field intensity, initial arc length, and arc current on the deflection of a welding arc in a magnetic field. The sensitivity characteristics of an arc sensor using magnetic arc oscillation were also analyzed for gas tungsten arc welding. First, a mathematical model of the magnetic arc deflection for theoretical prediction was introduced, then the model was confirmed by corresponding experiments. Finally, a model of an arc sensor using magnetic arc oscillation was set up mathematically by considering the model of magnetic arc deflection and electromagnet, as well as welding arc and welding power source. Experiments and simulations were carried out to investigate how welding conditions such as initial arc length and arc current affect the sensitivity of the arc sensor. The simulated results based on the model showed good agreement with experimental ones.

Introduction

A magnetic field externally applied to the welding arc deflects the arc by electromagnetic force (Lorentz force) in the plane normal to the field lines. The magnetic field exerts force on the electrons and ions within the arc, which causes the arc to be deflected away from the normal arc path. The welding arc can be deflected forward, backward, or sideways with respect to electrode and welding direction, depending upon the direction of an external magnetic field. A transverse magnetic field deflects the arc in the welding direction, whereas a longitudinal magnetic field deflects the arc perpendicular to the bead. If unidirectional magnetic field is applied to an AC arc, or an alternating field is applied to a DC arc, then the arc can be oscillated in the position normal to the direction of welding. This has been used to improve welding with both gas tungsten arc welding (GTAW) and gas metal arc welding (GMAW) processes (Ref. 1).

Deminskii, et al. (Ref. 2), conducted experiments using a GMAW process on an aluminum-magnesium alloy while a longitudinal magnetic field was applied to the welding arc. The magnetic fields applied were alternating and of the order of 40 gauss. They reported the arc oscillated across the weld axis. They also applied an alternating, transverse magnetic field to the welding arc. It was reported this resulted in a change in the shape of the weld pool. Not only was the solidification affected but the mechanical properties were improved by the application of a magnetic field to the gas metal arc welding of aluminum and magnesium alloys.

Serdyuk, et al. (Ref. 3), reported the metal transfer when magnetic arc oscillation was applied to gas metal arc welding. Images of the metal transfer indicated the droplets were emitted from the electrode at the moment of maximum arc deflection and the path of the molten drop was the same as the direction of the arc deflection just prior to the time the drop was detached from the electrode.

Oscillating the arc sideways with respect to welding direction could be used for strip cladding (Ref. 4) and welding of a material that is sensitive to hot cracking (Ref. 5), because this gives a wide bead and uniform and shallow penetration. The results indicate encouraging trends in increasing the melt-off rate/bead height by 15% and decreasing joint penetration by 20%, and hence dilution by 23%. No significant improvement in bead characteristics was observed by increasing peak magnetic flux density beyond 40 gauss. Metallographic examination (Ref. 5) of the solidification substructure showed arc oscillation decreases the size of the solidification substructure and thus provides a more desirable pattern of microsegregation in the weld metal. In general, increasing either the frequency or the amplitude of arc oscillation had an advantageous influence on the weld metal microstructure. This was found to be true whether the oscillation was performed parallel or perpendicular to the welding direction.

Subjecting the welding arc to transverse magnetic fields has beneficial effects only when the arc is deflected forward with respect to the direction of electrode travel (Refs. 6, 7). Applying an optimum magnetic field to a welding arc on both nonmagnetic and magnetic materials increases welding speed several times at which undercut-free and no-porosity welds can be made.

It is known the extent of arc deflection is dependent upon the flux density of the applied magnetic field, the arc current, arc length, and so on (Refs. 6, 8, 9). To apply magnetic arc oscillation to welding automation such as weld quality control and joint tracking, therefore, quantitative information has to be obtained about the effect of welding conditions on arc deflection.

Mathematically and empirically developed expressions of arc deflection, by Bachelis and Kovalev, respectively, incor-

---

Y. H. KANG and S. J. NA are with the Dept. of Mechanical Engineering, KAIST, Taejon, Korea.

KEY WORDS

Magnetic Arc
Deflection/Oscillation
Arc Physics
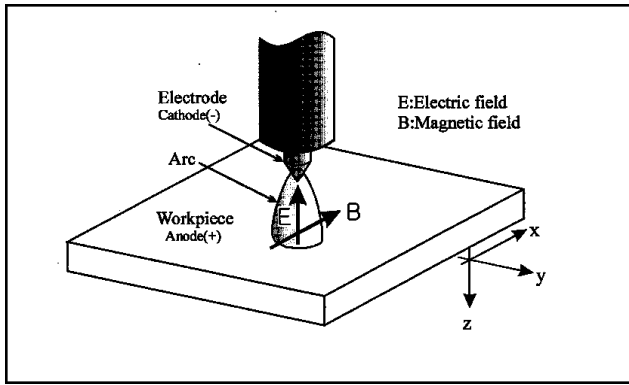Weld Process Simulation
Arc Sensor
GTAW

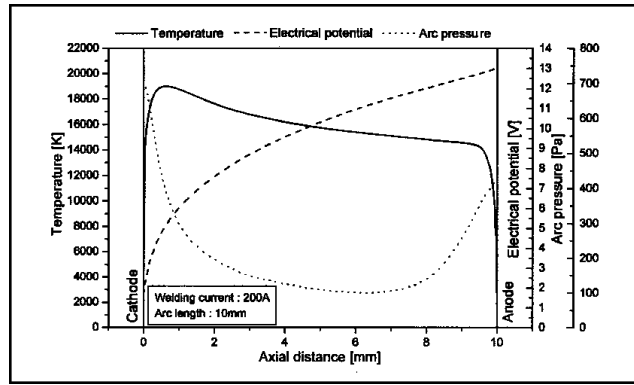Fig. 1 — Magnetic field externally applied on the welding arc.

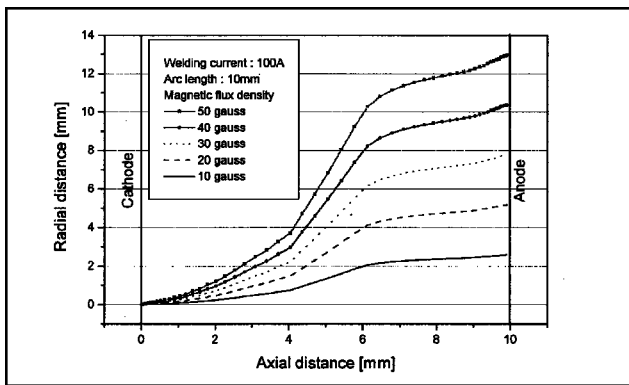Fig. 2 — Distributions of temperature, electrical potential, and arc pressure along the arc axis.

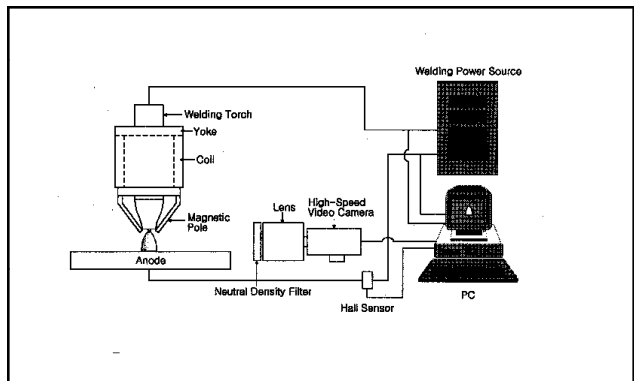Fig. 3 — Arc deflection calculated for various external magnetic flux densities.

Fig. 4 — Experimental setup for measurement of magnetic arc deflection.

porate similar dependencies, i.e., on initial arc length (l_o), magnetic field intensity (H) and arc current (i) (Refs. 8, 9). These relationships are as follows:

$$\delta = \frac{ci}{4H}\left[1 - \left(1 - \frac{16H^2 l_o^2}{c^2 i^2}\right)^{1/2}\right] \quad \text{and}$$

$$\delta = \frac{kH l_o^2}{\left(i^2 - k^2 H^2 l_o^2\right)^{1/2}}$$

(1)

where c and k are dimensionless constants representing arc rigidity and   is the arc deflection measured by the movement of the center of the anode spot with the application of a magnetic field. Because the rigidity constants are usually unknown, these equations have found little practical use.

The arc sensor is based on a sensing technique developed by using a fundamental arc property, which is that arc current and voltage characteristics vary with variations in torch height (electrode extension length + arc length). The practical advantages, such as the absence of any welding torch and robot arm additions, its

status as a cheap and simple technique, good real-time operability, and little susceptibility to the effect of electrode wire bending, have made this approach eminently applicable to automatic joint tracking (Refs. 10–12).

Weaving frequency of mechanical units such as a robot arm is limited to about 10 Hz because the inertia of the arm and welding torch causes overshoot and dynamic instability of the system. Therefore, real-time joint tracking using a mechanically induced weaving method limits the attainable welding speed. But magnetic arc oscillation could be applied to high-speed joint tracking because the magnetically oscillating arc possesses virtually no inertia and a weaving frequency of up to 200 Hz is permitted (Ref. 1). The magnetic arc oscillation method easily controls weaving width and frequency by the control of magnitude and frequency of applied current to the electromagnet. The frequency of oscillation of the arc is the same as that of the controlling magnetic field.

In this study, a mathematical model of magnetic arc deflection was introduced

for theoretical prediction; the model was confirmed by corresponding experiments. Also, the effects of magnetic field intensity, initial arc length, and arc current on the deflection of the gas tungsten welding arc in a magnetic field were investigated. The arc sensor using magnetic arc oscillation was also modeled mathematically by considering the model of magnetic arc deflection and electromagnet as well as the welding arc and welding power source. Experiments and simulations were carried out in order to clarify how welding conditions affect the sensitivity characteristics of the arc sensor.

Model of Magnetic Arc Deflection

Since electron density n_e is approximately equal to that of ions n_i in the column of an arc plasma except where very close to the electrodes, the welding arc can be assumed to be electrically neutral, or $n_e \approx n_i$ (= n). Mass density   , charge density s, mass velocity u , and current density j in an arc plasma satisfying a electrically neutral condition are therefore expressed as follows:
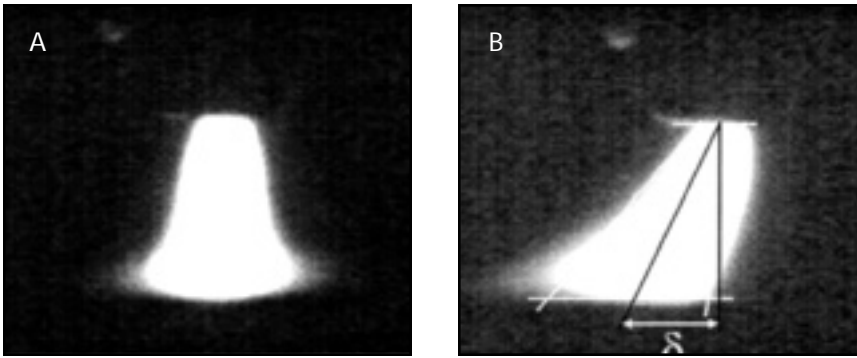
Fig. 5 — Arc column images captured by high-speed camera. A — Undeflected arc column; B — arc column deflected by constant magnetic field.

Table 1 — Physical Constants Used in Calculating Arc Deflection

Electronic charge	$q = 1.602 \times 10^{-19}$ coulomb
Boltzmann constant	$k = 1.38 \times 10^{-23}$ J/K
Electronic mass	$m = 9.108 \times 10^{-31}$ kg
Permittivity of free space	$\epsilon_o = 8.854 \times 10^{-12}$ farad/m

Table 2 — Experimental Conditions

Welding current	100–300 A
Arc length	5–10 mm
Magnetic flux density	0–7 gauss
Shielding gas	Pure Ar
Electrode	2.4- mm-diameter, 60-deg thoriated tungsten

$$\rho = n_i M + n_e m \approx n(M+m) \approx nM \quad (2)$$

$$\rho_c = (n_i - n_e)q \quad (3)$$

$$u = \frac{n_i M u_i + n_e m u_e}{\rho}$$

$$= \frac{M u_i + m u_e}{M + m} \approx u_i + \frac{m}{M} u_e \quad (4)$$

$$j = q(n_i u_i - n_e u_e) \approx nq(u_i - u_e) \quad (5)$$

where m, M are the electron and ion mass respectively, u_i the ion velocity, the u_e electron velocity, and q the electronic charge.

Generally, arc plasma consists of uncountable electrons and ions, so the equations of motion about electron and ion have to be solved separately to calculate the motion of plasma. In highly ionized plasma, coulomb collisions dominate over collisions with neutral atoms. Thus, the two momentum balance equations only considering the coulomb collisions are referred to as the individual fluid equations of motion.

$$Mn_i \frac{d u_i}{dt} = qn_i (E + u_i \times B) - \nabla p_i + R_{ie}$$

$$mn_e \frac{du_e}{dt} = qn_e (E + u_e \times B) - \nabla p_e + R_{ei} \quad (6)$$

where E, B are the electric and magnetic field, p_i, p_e the ion and electron pressure and R_{ie} and R_{ei} describe the collisional transfer of momentum between two species (Ref. 13). These two equations are added together, to produce the combined equation of motion.

$$\rho \frac{d u}{dt} = \rho \left(\frac{\partial u}{\partial t} + u \cdot \nabla u \right) =$$

$$\sigma E + j \times B - \nabla p \quad (7)$$

where $p = p_e + p_i$ is the total pressure. In adding the two individual fluid equations of motion, the collision terms cancel each other since $R_{ie} = -R_{ei}$.

In practice, however, mass velocity of a plasma is generally dominated by the ions, being much heavier than the electrons, so there is no distinction between u and the ion mean velocity u_i. Momentum transfer from ions to electrons is expressed in terms of velocity difference and average collision frequency (or, the plasma resistivity η).

$$R_{ei} = mn \langle \nu_{ei} \rangle (u_i - u_e) =$$

$$\eta n^2 q^2 (u_i - u_e) = \eta nq \, j \quad (8)$$

Welding arc plasma can be assumed to be electrically neutral. So, Equation 7 may be rewritten

$$E + u \times B = \eta \, j + \frac{j \times B - \nabla p_e}{nq} \quad (9)$$

Also, the diffusion by external magnetic field can be assumed to be a sufficiently static process that the plasma is always in a state of equilibrium. These assumptions allow us to neglect the inertia of the ions as well as that of electrons, and to replace Equation 7 as follows:

$$j \times B = \nabla p \quad (10)$$

Assuming the external magnetic field B_x is only in the x-direction and the pressure gradient dp/dz and the electric field E_z are only in the z-direction, then the equations of perpendicular components of the plasma velocity are obtained from Equations 9 and 10 as follows:

$$u_y = \frac{E_z}{B_x} - \frac{1}{2nqB_x} \frac{dp}{dz}$$

$$u_z = -\frac{\eta}{B_x^2} \frac{dp}{dz} \quad (11)$$

Equation 11 can be used only in calculating the diffusion perpendicular to a magnetic field in highly ionized plasma. Arc deflection is, therefore, as follows:

$$\delta = \frac{u_y}{u_z} z = \frac{E_z - \frac{1}{2nq} \frac{dp}{dz}}{-\eta \frac{dp}{dz}} B_x \, z \quad (12)$$

where z is the axial distance. Equation 12 shows the magnitude of magnetic arc deflection is linearly proportional to the external magnetic flux density.

The external magnetic field applied on arc plasma was assumed to be uniform and only in x-direction perpendicular to the electrode axis as shown in Fig. 1. The coordinate system shown in Fig. 1 indicates x is the direction of welding, y is transverse to welding direction in the plane of the workpiece, and z coincides with the axis of the electrode. Distributions of pressure gradient, temperature, and electric field in the arc plasma were obtained by numerical analysis of the gas tungsten welding arc under argon shielding gas by using a code based on a finite difference method developed in an earlier study (Ref. 14). In the study, a two-dimensional, steady-state mathematical model of the arc assuming the current density distribution along the cathode surface was applied to GTAW in an argon atmosphere for investigating the influences of parameters such as electrode angle, welding current, and arc length on the welding arc. The current density distribution was assumed to have a Gaussian form characterized by the maximum current density at the electrode tip or the dis-
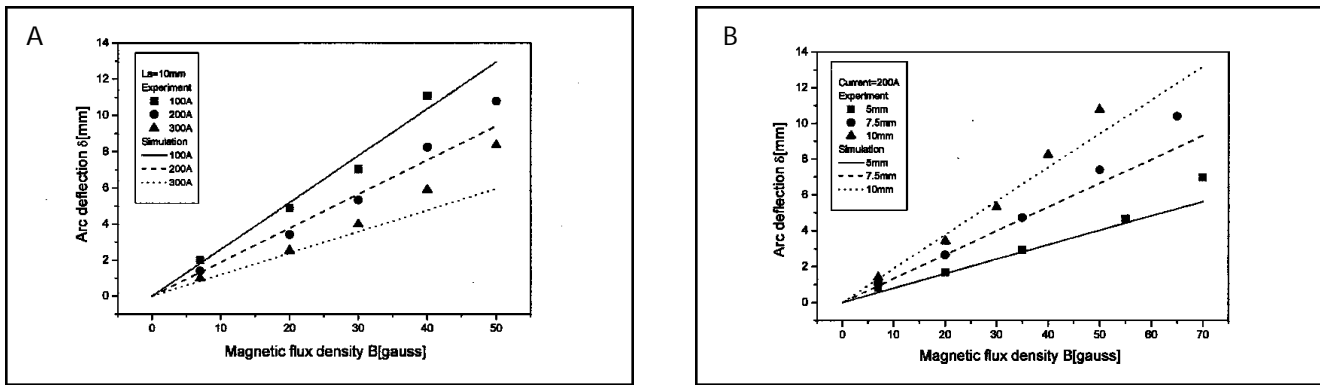
Fig. 6 — Calculated and experimental results of arc deflection. A — Effects of externally applied magnetic flux density on arc deflection for various welding currents; B — effects of externally applied magnetic flux density on arc deflection for various arc lengths.
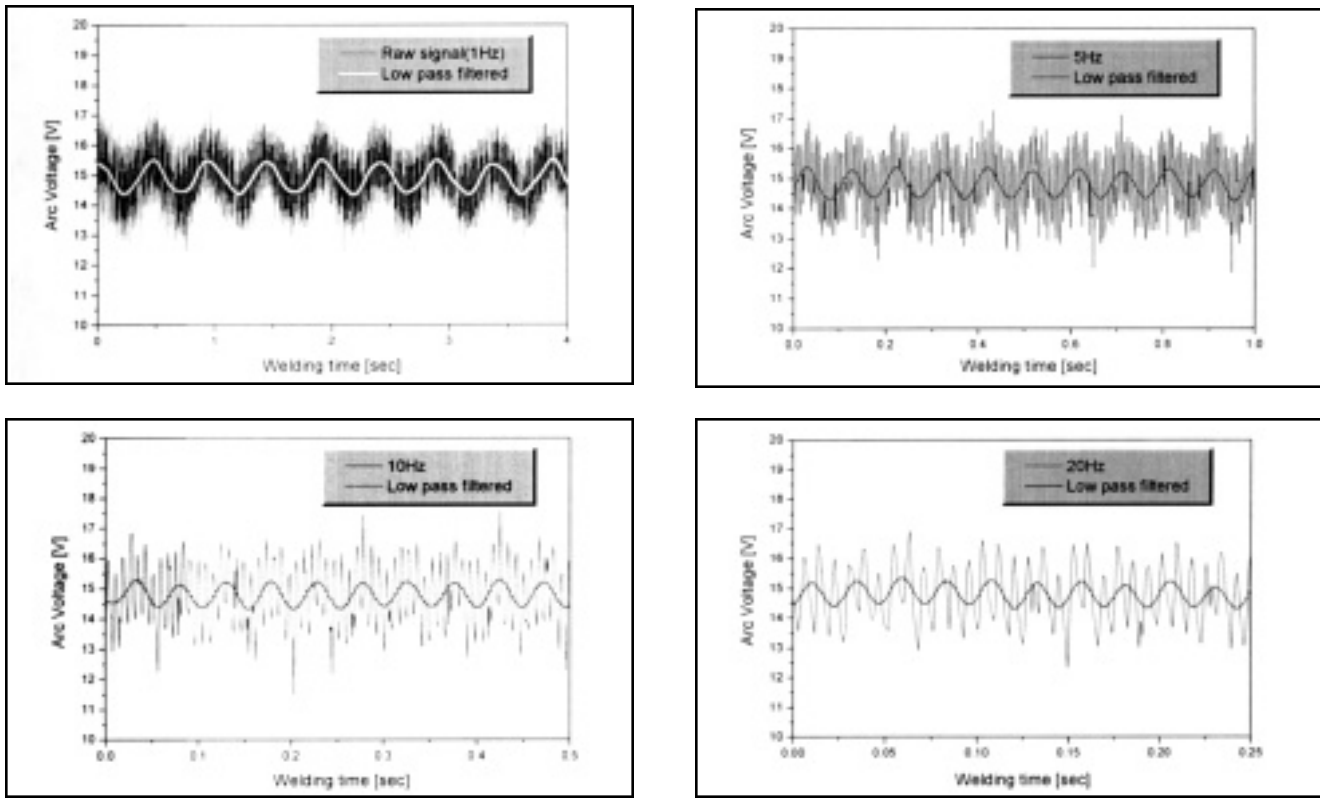

Fig. 7 — Welding voltage waveforms with magnetic arc oscillation for various oscillation frequencies.

tribution parameter. Because the electrode shape is curved and the size small compared to the arc region, it is difficult to represent electrode configuration by the rectangular grid. Thus, a boundary-fitted coordinate system was adopted to precisely describe the electrode surface. A more detailed description of the mathematical model can be found in the earlier publication (Ref. 14). For this investigation, the numerical analysis of a gas tungsten welding arc under argon shielding gas was carried out for a welding current of 100 ~ 300 A, arc length of 5 ~ 10 mm and electrode angle of 60 deg. Figure 2 shows distributions of pressure gradient, temperature, and electric field along the arc center axis with a welding current of 200 A and an arc length of 10 mm. Arc pressure and temperature near the cathode are higher than near the anode (Refs. 14, 15). A steep gradient of electrical potential near the cathode tip results in high current density, which generates a strong magnetic force. This strong magnetic force acting upon the welding arc generates a steep pressure gradient near the cathode tip, which in turn accelerates the argon plasma toward the anode plate.

Physical constants used in calculating arc deflection are shown in Table 1. Figure 3 shows the calculated results of arc centerline deflection for various magnetic flux densities with a 100-A welding current and 10-mm arc length. Although the deflection of arc centerline increased nonlinearly with axial location from cathode tip to anode plate, total deflection increased almost linearly with magnetic flux density. As shown in the figure, the magnitude of deflection at an axial distance halfway between the electrode and
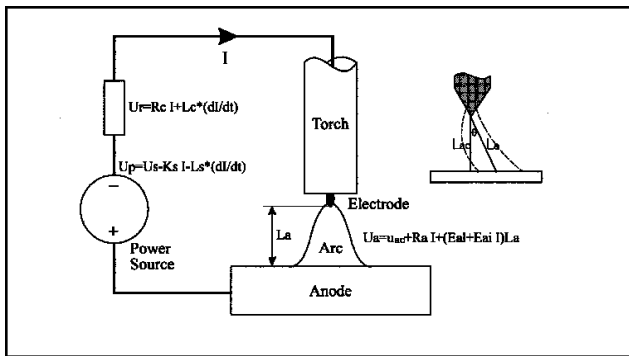
Fig. 8 — Equivalent circuit of GTAW system with constant current power source.

Fig. 9 — Comparison of welding voltage waveform obtained by simulation and experiment during magnetic arc oscillation
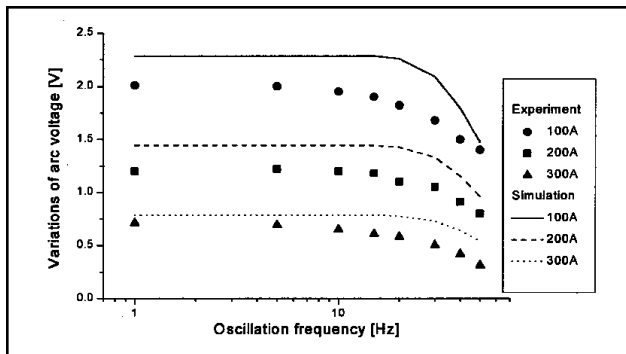

Fig. 10 — Experimental and theoretical frequency characteristics of arc sensor during bead-on-plate welding with magnetic arc oscillation.

workpiece was much more than at the vicinity of the cathode and anode.

Experiment of Magnetic
Arc Deflection

To verify the model of magnetic arc deflection, corresponding experiments were carried out under various welding conditions as listed in Table 2. Figure 4 shows the experimental apparatus of GTA welding for investigating the extent of arc deflection. The water-cooled copper anode, which would not melt during welding, was used in the experiments for generating a constant and stable arc. The copper-anode was cooled down by a forced water flow to prevent it from rising above its melting temperature. The magnitude of magnetic arc deflection was measured with a high-speed video camera. Figure 5 shows the characteristic images of undeflected arc column and deflected arc column by a constant magnetic field as captured by the high-speed camera. The magnitude of the deflection is defined as the offset of arc centerline at the anode plate, as shown in Fig. 5B.

Figure 6 shows the effects of exter-

nally applied magnetic flux density on arc deflection for various welding currents and arc lengths. As the magnetic flux density and arc length increase, the magnitude of arc deflection also increases, while it decreases with increasing welding current. This is probably due to the fact an increase in current and a decrease in arc length makes arc stiffness increase. In Fig. 6, calculated arc deflections based on the model were compared with experimental ones. Although magnetic flux density and arc deflection were related linearly in the calculated results, they showed a nonlinear relation in the experimental ones. The linear relationship between magnetic flux density and arc deflection is probably attributable to the calculation that considered only the centerline deflection. Consequently, the proposed model can't represent the nonlinearity of experiments with sufficient exactness.

Variation of Welding Voltage with
Magnetic Arc Oscillation

Magnetic arc oscillation changes arc length, which periodically changes the welding voltage and current. An alternating parallel magnetic field causes the arc to oscillate in position normal to the direction of welding, which takes effect like a mechanical weaving. There is, however, a difference between magnetic arc oscillation and mechanical weaving on the flat plate. In mechanical weaving, the welding

voltage and current are constant during bead-on-plate welding, while in magnetic arc oscillation they change periodically. The welding voltage variation was investigated during bead-on-plate GTA welding using magnetic arc oscillation.

Figure 7 shows the raw and filtered welding voltage signals for various oscillation frequencies during bead-on-plate welding. As shown in the figure, the signals consist of two frequency components: a high-frequency noise component varying faster than the arc oscillation and a basic signal component varying at the same frequency as the arc oscillation. Although the ripple voltage of a welding power source is about 2–3 V, the welding voltage fluctuation still shows the magnetic arc oscillation clearly. The arc sensor makes use of the basic signal components in these waveform signals. The basic signal components were therefore extracted by a digital low-pass filter. In Fig. 7, the solid line marks the waveform after low-pass filtering. This welding voltage variation can be used for the output signal of the arc sensor.

The arc sensor using magnetic arc oscillation was mathematically modeled for theoretical prediction. Figure 8 shows the equivalent electrical circuit of a conventional GTA welding system composed of a welding power source, welding arc, and cables. A conventional welding power source can be considered as generally equivalent to a constant U_s source with an output resistance K_s and inductance L_s. The welding cable is also characterized by its resistance R_c and inductance L_c. The arc voltage U_a consists of voltage drops in the anodic zone, cathodic zone, and arc column. Based on the experimental results, it is characterized by a constant component u_{ao}, resistance R_a, and elec-
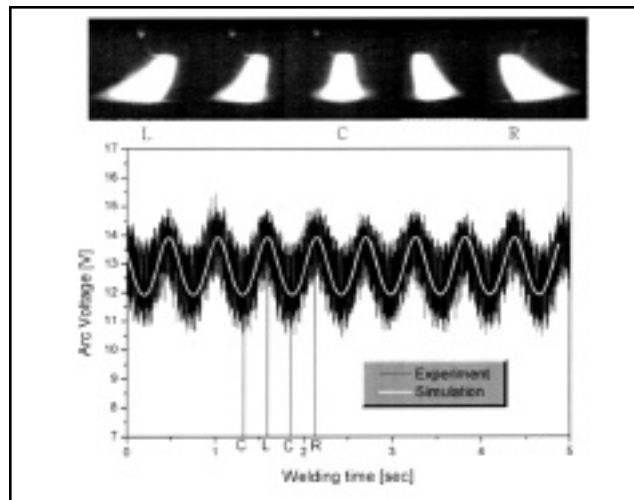
tric field intensity E_a (= E_{al} + $E_{ai}I$) of arc column. Thus, the voltage equations for the whole loop of welding circuit can be written as follows:

$$\frac{dI}{dt} = \frac{U_s - u_{ao}}{L_s + L_c} - \frac{K_s + R_c + R_a}{L_s + L_c} I$$
$$- \frac{E_{al} + E_{ai}I}{L_s + L_c} L_a \tag{13}$$

where I is the welding current and L_a the arc length (Ref. 12). As shown in Fig. 8, the arc length L_a is expressed as a function of deflection angle and can be written as follows:

$$L_a = \frac{L_{ao}}{\cos\theta} \tag{14}$$

where L_{ao} is the initial arc length.

With increasing the alternating frequency of voltage applied to the electromagnet coil, the current through the coil decreases gradually due to the coil inductance, which means the magnetic flux density generated from the electromagnet also decreases. Finally, the arc deflection and the welding voltage variation are lowered. This phenomenon was taken into account for simulation of the arc sensor.

Figure 9 shows the experimental and calculated results of welding voltage variation when magnetic arc oscillation is used. L and R represent the left and the right end position of the arc, while C refers to the central position in the arc oscillation. The voltages were maximized both at L and R and minimized at C due to the variation of arc length. The difference between maximum and minimum voltage, or the variation amplitude of welding voltage, was about 2 V. The simulation result was in a fairly good agreement with the experimental one.

Figure 10 shows the variations of welding voltage sensitivity for various oscillation frequencies and welding currents. The low-pass filtering technique was used in experimental results to ensure a correct determination of the welding voltage variation amplitude. The variation increased with the decrease of welding current at the same magnetic flux density because of the increase in arc deflection. As the oscillation frequency increased, the magnetic flux density generated from the electromagnet was reduced due to the electromagnet inductance, as discussed above. In the case of the electromagnet used in the present work, the magnetic flux density decreased remarkably at an oscillation frequency of more than 15 Hz. Consequently, welding voltage variations were reduced considerably over 15 Hz, as shown in Fig. 10. If the reduction of magnetic flux density can be compensated, the variation, or sensitivity,

of the arc sensor will likely remain almost constant even over a 15-Hz oscillation frequency.

Conclusions

Through the simulation and experiment of magnetic arc deflection and arc sensor using magnetic arc oscillation, the following conclusions were obtained:

1) A magnetic arc deflection model considering only arc centerline deflection was obtained. From the experimental and simulation results, it was found magnetic flux density and arc deflection are related linearly in lower magnetic flux density for both results.

2) The magnetic arc oscillation resulted in a change of arc length, which in turn made the welding voltage signals periodically change in GTAW. Although the signals included ripple voltage of the welding power source (high-frequency noise component) of about 2–3 V, the welding voltage fluctuation (the basic signal component) produced by the magnetic arc oscillation was clearly shown. The basic signal components were, therefore, extracted by a digital low-pass filter, which can be used for the output signal of the arc sensor.

3) Due to inductance, the magnetic flux density generated from the electromagnet was gradually reduced with an increase of oscillation frequency. It is necessary to compensate for the reduced magnetic flux density to maintain a constant sensitivity of the arc sensor in the whole frequency range.

References

1. Hughes, R. V., and Walduck, R. P. 1987. Electromagnetic arc path control in robot plasma welding. Robotic Welding. IFS Publication and Springer-Verlag, pp. 243–263.

2. Deminskii, Y. A., and Dyatlov, V. I. 1963. Magnetic control during gas shielded arc welding with a consumable electrode. Automatic Welding (4): 67–68.

3. Serdyuk, D. B., and Kornienko, A. N. 1963. The welding arc in an alternating transverse magnetic field. Automatic Welding (10): 7–13.

4. Mallya, U. D., and Srinivas, H. S. 1993. Magnetic steering of arc and bead characteristics in submerged arc strip cladding. Welding Journal 72(11): 517-s to 522-s.

5. Tseng, C. F., and Savage, W. F. 1971. The effect of arc oscillation. Welding Journal 50 (11): 777-s to 786-s.

6. Hicken, G. K., and Jackson, C. E. 1966. The effect of applied magnetic fields on welding arcs. Welding Journal 45(11): 515-s to 524-s.

7. Jayarajan, T. N., and Jackson, C. E. 1972. Magnetic control of gas tungsten arc welding process. Welding Journal 51(8): 377-s to 385-s.

8. Ecer, G. M. 1980. Magnetic deflection of the pulsed current welding arc. Welding Journal 59(6): 183-s to 191-s.

9. Lancaster, J. F. 1986. The Physics of Welding. Oxford, Pergamon.

10. Sugitiani, Y., Kobayashi, Y., and Murayama, M. 1991. Development and application of automatic high speed rotation arc welding. Welding International 7(5): 577–583.

11. Cook, G. E., Barnett, R. J., Andersen, K., and Strauss, A. M. 1995. Weld modeling and control using artificial neural networks. IEEE Trans. Ind. Applicat. 31(6): 1484–1491.

12. Ushio, M., and Mao, W. 1996. Modeling of an arc sensor for DC MIG/MAG welding in open arc mode: study of improvement of sensitivity and reliability of arc sensors in GMA welding (1st Report). Q. J. Jpn. Weld Soc. 14(1): 99–107.

13. Goldston, R. J., and Rutherford, P. H. 1995. Introduction to Plasma Physics. Bristol and Philadelphia, Institute of Physics Publishing.

14. Lee, S. Y., and Na, S. J. 1996. A numerical analysis of a stationary gas tungsten welding arc considering various electrode angles. Welding Journal 75(9): 269-s to 279-s.

15. Hsu, K. C., Etemadi, K., and Pfender, E. 1983. Study of the free-burning high-intensity argon arc. J. Appl. Phys. 54(3): 1293–1301.